Wideband Loop Antenna with Electronically Switchable Circular Polarization

Long Zhang, Steven Gao, Member, IEEE, Qi Luo, Member, IEEE, Paul Young, Senior Member, IEEE, Qingxia Li, Member, IEEE

Abstract—This paper presents a novel printed antenna which achieves wide bandwidth, high gain and reconfigurable circular polarizations. A loop antenna is printed on both sides of a dielectric substrate: a dual PIN diode loaded loop is printed on one side while a dual gap loaded smaller loop is etched on the other side. By controlling the on/off states of the PIN diodes, the polarization of the proposed antenna can be switched electronically to right-hand circular polarization (RHCP) or left-hand circular polarization (LHCP) over a wideband frequency range. A prototype is fabricated and measured to verify the performance of the antenna. The measured results indicate that the antenna can achieve an impedance bandwidth of over 30%, and a 3-dB axial ratio (AR) bandwidth of 12.7% and 14.9% for RHCP and LHCP, respectively. The measured gain is around 8 dBic for LHCP state and 7 dBic for RHCP state. Due to advantages of wide overlapped bandwidth, simple feeding structure and high gain, this antenna is promising for applications in dual-CP wireless communication systems.

Index Terms—Loop antennas, circular polarization, reconfigurable antennas, impedance matching.

I. Introduction

RECENTLY polarization reconfigurable antennas have received considerable interest since they are useful for many applications, such as polarization diversity, synthetic aperture radar (SAR) systems, frequency reuse, sensor systems, mitigation of multipath effects, etc [1, 2].

It is stated in [3] that the channel capacity of a 2 × 2 MIMO orthogonal frequency division multiplexing (OFDM) system is improved by using circularly polarized reconfigurable antennas compared with the single polarization system. A more comprehensive experiment held in [4] has shown that polarization reconfigurable antennas used in conjunction with adaptive space–time modulation techniques provide additional degrees of freedom to MIMO systems, resulting in more robust system. These studies have verified experimentally the benefits of deploying polarization reconfigurable antennas.

Compared with linearly polarized antennas, circularly polarized antennas have several advantages such as the mitigation of multi-path fading, the immunity of 'Faraday rotation' and the reduction of polarization mismatching between transmitting and receiving antennas [5]. Therefore, antennas with switchable circular polarizations have been widely investigated. For example, a PIN diode controlled U-slot patch antenna was proposed in [6]. A piezoelectric transducer (PET) based antenna with similar functionality was designed in [7]. However, the 3-dB axial ratio (AR) bandwidths of these two antennas are relatively narrow. An E-shaped polarization reconfigurable patch antenna presented in [8] can achieve a 7% overlapped bandwidth while 10% bandwidth is obtained in [9]. The L-probe feeding structure used in [9], however, increases the complexity of the antenna. A polarization reconfigurable loop antenna was reported in [10]. This antenna can only switch its polarization states between linear polarization and RHCP. Furthermore, the VSWR is larger than 2.5 when the RHCP wave is radiated.

In this letter, a printed loop antenna with switchable circular polarizations is presented. A parasitic dual-gap loaded loop is introduced inside the primary loop in order to improve the bandwidth of the antenna. Compared to the other reported polarization reconfigurable antennas, the presented design achieves wider overlapped bandwidth with a simple configuration.

II. Antenna Configuration and Operation Principles

A. Antenna Configuration

The configuration of the proposed antenna is shown in Fig. 1. As shown, two loops are printed on both sides of a 0.8mm ×100mm×100mm Rogers RO4003C substrate with dielectric constant of 3.55 and dissipation factor of 0.0027. The outer loop is loaded by two PIN diodes and is printed on the top layer of the substrate. The inner loop with two small gaps is etched on the bottom layer of the substrate. Beneath the antenna board, there is a ground plane with the size of 150mm×150mm which reflects the downward waves to achieve directional radiation pattern.

There are also two magnified pictures in Fig. 1 (a) showing the specific control mechanism of PIN diodes and DC blocking. Regarding the control of the PIN diodes, two DC bias lines are introduced with a small square pad for soldering. Inductors with values of 33nH are inserted into the DC bias lines for RF choking while the DC blocking is implemented by two 5.6 pF capacitors built in the feed line.

L. Zhang, S. Gao, Q. Luo and P. R. Young are with the School of Engineering and Digital Arts, University of Kent, Canterbury CT2 7NT, UK. (emails: lz76@kent.ac.uk; s.gao@kent.ac.uk).

Q. Li is with the School of Electronic Information and Communications, Huazhong University of Science and Technology, Wuhan 430074, China.

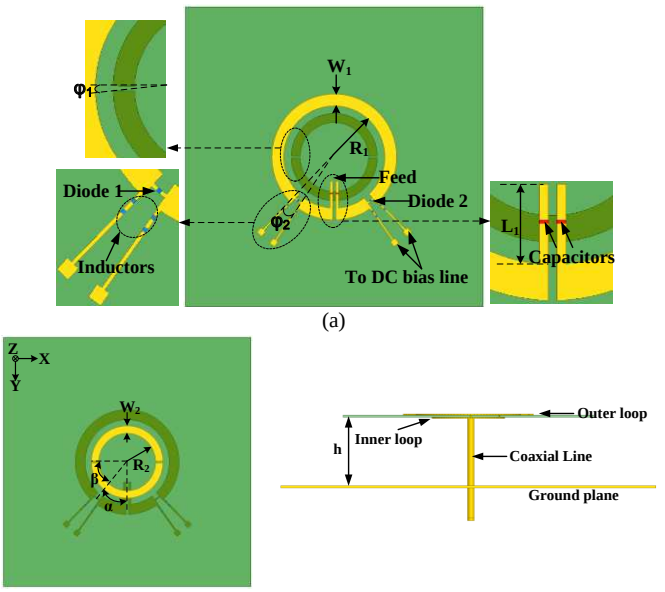

Fig. 1. Configuration of the proposed antenna: (a) top view, (b) bottom view, (c) side view.

The circumferences of the two loops are designed to be approximately one wavelength at the lower (2.4GHz) and higher frequencies (2.8GHz). The antenna height h is around 0.2λ -0.25λ where λ is the free space wavelength at 2.4GHz. Changing this height affects not only the directional radiation but also the CP characteristics [11]. The optimized antenna dimensions are shown in TABLE I.

TABLE I
ANTENNA DIMENSIONS

R_1	R_2	W_1	W_2	L_1	φ_1	φ_2	α	β	h
17mm	11.5mm	4mm	3mm	9mm	3°	7°	40°	50°	27.2mm

B. Operation Principles

It is well known that a one-wavelength loop antenna radiates a linearly polarized wave. By introducing a gap within a circular loop antenna a traveling wave current is excited and thus circularly polarized radiation can be achieved [12].

Since the PIN diodes act more like capacitors when they are reversely biased, it is therefore feasible to use PIN diodes to control the direction of the current along a CP loop antenna. More specifically, as shown in Fig. 1, two PIN diodes are integrated into a circular loop at symmetric positions. When PIN diode 1 is turned on and PIN diode 2 is off, there is a travelling-wave current flowing in clockwise direction resulting in a LHCP wave in the far-field. Conversely, when PIN diode 1 is off and the other one is on, a RHCP wave is radiated. Through controlling the states of these two PIN diodes, a CP loop antenna with electronically switchable circular polarization is obtained.

C. AR Bandwidth Enhancement for Dual-CP Loop

It has been found that the AR bandwidth of a CP loop antenna can be enhanced by adding a smaller parasitic open loop inside the original one [13, 14]. The concept is to create another minimum AR point beyond the original minimum AR point produced by a CP loop without any parasitic structures. By appropriately combing these two minimum AR points, the CP bandwidth can be enhanced significantly.

Unlike conventional CP loop antennas with only single-sense circular polarization, the AR bandwidth enhancement for dual-sense CP loop antenna is different. It is no longer feasible to improve the AR bandwidth of a dual-sense CP loop antenna by simply adding a single-gap loaded parasitic loop. If a parasitic loop with only one gap near PIN diode 1 is placed inside the primary loop shown in Fig. 1, the AR bandwidth under RHCP state can be enhanced. However, the AR bandwidth of LHCP cannot be improved since the distance between the gap and the PIN diode 2 is too large to compensate the magnitude variation of the current on the primary loop. Therefore, in order to improve the bandwidth of the antenna under both RHCP and LHCP states, a double-gap loaded parasitic loop is placed inside the primary loop.

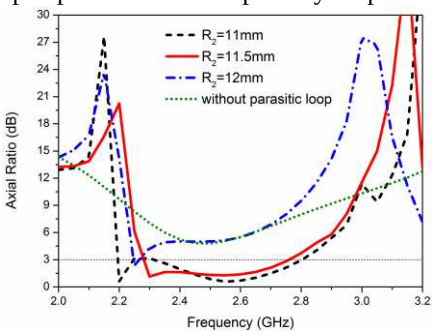

Fig. 2. Axial ratio variation with different R_2 under LHCP state.

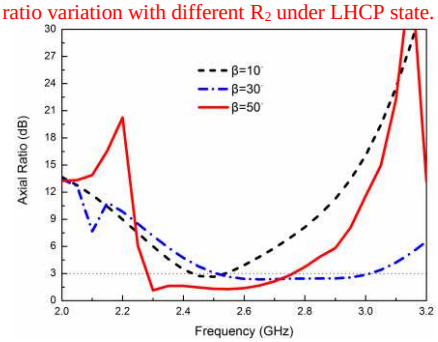

Fig. 3. Axial ratio variation with different β under LHCP state.

Fig. 2 and Fig. 3 show the AR variation with different values of R2 and β, respectively. In these two figures, only one parameter is changed while the other parameters are keeping unchanged as in Table I. Fig. 2 also shows the AR without a double-gap loaded parasitic loop under LHCP state. It is found that the axial ratio is larger than 3 dB when the double-gap loaded parasitic loop is not existed. Compared with the result observed in [14], where the AR is still less than 3 dB even with the parasitic loop is removed. It is concluded that the dual-gap loaded parasitic loop is different from single-gap loaded parasitic loop in helping compensate the magnitude variation of the current on the primary element. As can be seen from these two figures, R2 and β can affect the CP performance of the proposed antenna. By changing them, the coupling between the parasitic loop and primary loop is varied, which will influence the electric currents flowing on each loop. Once the optimal

values of R2 and β are chosen, travelling-wave electric current can be generated and good CP performance is achieved.

III. Results and Discussion

A. Reflection Coefficient

The prototype of the proposed antenna is shown in Fig. 4. As can be seen from the figure, four DC biased lines are soldered perpendicularly to the antenna board and then connected to the single-pole double-throw (SPDT) switch for controlling the two PIN diodes. Through shielding the DC lines and the switch by ground plane, the influence caused by DC biased lines and switches can be minimized. Besides, there are also ferrite beads placed along the coaxial cable, which are used to minimize current flowing on the outside of the cable.

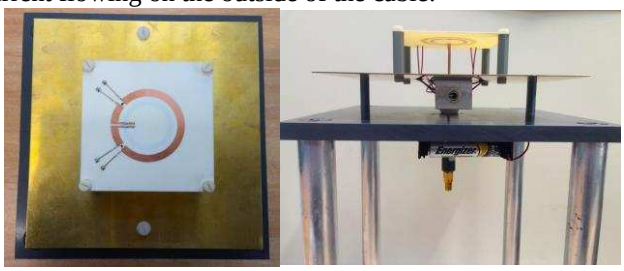

(a) (b)

Fig. 4. Prototype of the proposed antenna: (a) top view, (b) side view.

Two Skyworks SMP1345-079LF PIN diodes with small capacitance (smaller than 0.2pf) and series resistance (2Ω) are used in the prototype. To drive the two PIN diodes, two batteries with 1.5V voltages are mounted in a battery bracket and then are connected to a SPDT switch. The polarization status of the presented antenna can be changed to LHCP or RHCP electronically by controlling the state of the switch.

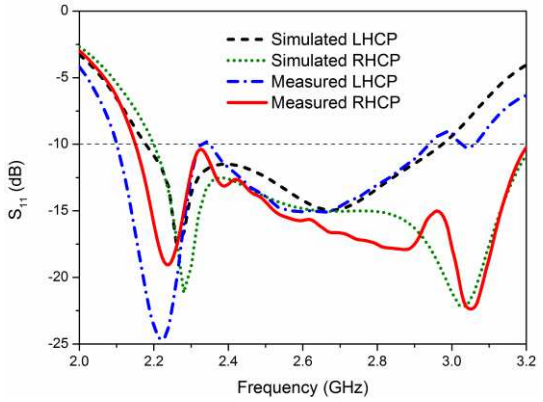

Fig. 5. Simulated and measured reflection coefficients.

As shown in Fig. 5, the experimental reflection coefficients and simulated ones are in good agreement. From the measured results, a 32% impedance bandwidth is achieved under LHCP state while a 38.8% bandwidth is obtained under RHCP state. The asymmetric LHCP and RHCP results are mainly caused by the unbalanced feeding coaxial cable. We have tried to use several baluns such as the sleeve balun and integrated slotline balun to conquer this issue. However, they are not suitable for the proposed antenna. The sleeve balun is a narrow-band structure which has little performance improvement to this antenna. The integrated balun is too big for this antenna which degrades the AR a lot as explained in [15]. Considering these practical issues, ferrite beads are finally used to relieve the current flowing along the outer conductor of the cable.

B. Axial Ratio

Fig. 6 (a) and (b) shows the measured and simulated AR under LHCP and RHCP states, respectively. As observed from the figure, the measured AR bandwidth is slightly smaller than the simulated results. The discrepancy between the simulation and measurement results may stem from the simplified equivalent circuit model of PIN diodes in the simulation model. Series inductance (L) and parallel resistance (RP) are not included in the simulation model and this may have some influences to the antenna's performance.

For a polarization reconfigurable antenna with CP polarizations, the overlapped bandwidth between impedance bandwidth and AR bandwidth is usually used to evaluate the antenna's bandwidth characteristic. Comparing Fig. 5 and Fig. 6, it is found that the measured overlapped bandwidth under RHCP and LHCP states is 12.7% and 14.9%, respectively.

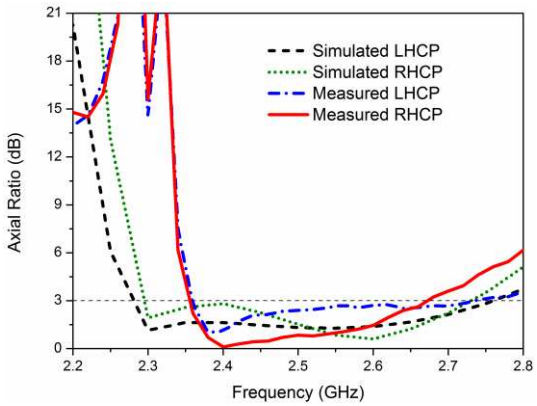

Fig. 6. Simulated and measured axial ratio.

C. Radiation Pattern and Antenna Gain

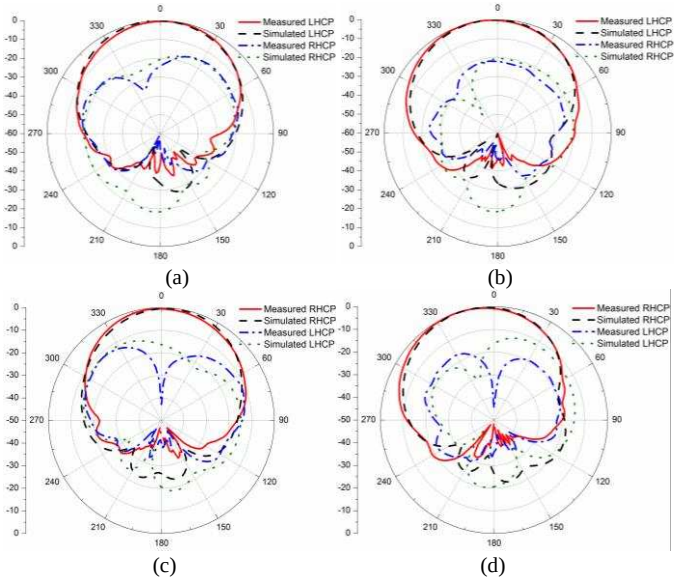

Fig. 7. Simulated and measured radiation patterns at 2.4GHz: (a) LHCP state, XoZ plane, (b) LHCP state, YoZ plane, (c) RHCP state, XoZ plane, (d) RHCP state, YoZ plane.

The radiation pattern of the proposed antenna is measured using a linearly polarized horn antenna and the method presented in [16] is employed to calculate the RHCP and LHCP radiation patterns. Fig. 7 shows the normalized radiation patterns under LHCP and RHCP states at 2.4GHz in two principle planes.

As shown in the figure, the measured radiation patterns are of good agreement with the simulation results. A unidirectional radiation pattern with low cross polarization can also be observed. The asymmetric radiation pattern may cause by the unbalanced feed and non-uniform current distribution along the circular loops. To avoid the reflection from the antenna holder, an absorber is mounted below the ground plane of the antenna under testing. The back radiation is absorbed by this absorber and thus the measured back lobe is very low. Considering that there is a ground plane under the proposed antenna and the main beam characteristic is of major concern, the measured radiation patterns can reveal these characteristics and thus are regarded to be able to evaluate the antenna's performance.

Fig. 8 gives out the simulated and measured gain of the proposed antenna. As can be seen, there is a sharp decrease of antenna gain at 2.3GHz. The ripple around 2.3GHz can also be observed from the S11 and AR figures. This may be caused by the diodes' characteristics and possible fabrication errors. Considering the antenna works as a CP antenna from 2.35 to about 2.7GHz, the gain is about 8dBic and 7dBic across the operation band for LHCP and RHCP states, respectively. The measured gain differences between LHCP and RHCP states are caused by the unbalanced feeding structure as explained in section III A.

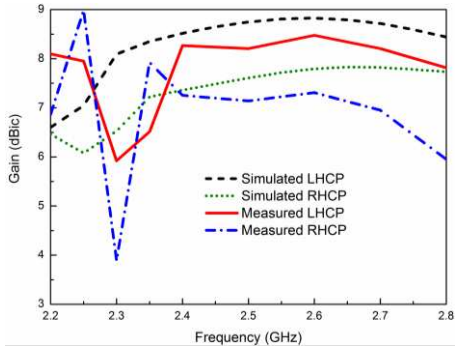

Fig. 8. Simulated and measurement gain under LHCP and RHCP states.

D. Comparison with Other Antennas

TABLE II
COMPARISON OF POLARIZATION RECONFIGURABLE ANTENNAS

Ref. No.	Impedance Bandwidth	Overlapped Bandwidth	Gain	Feeding Complexity	Antenna Size
[7]	13.5%	2.8%	7 dBic	simple	0.77λ×0.77λ×0.06λ
[8]	2.6%	< 1%	5.4 dBic	simple	-
[9]	7%	7%	6-8 dBic	simple	1.63λ×0.82λ×0.08λ
[10]	25.4%	10%	6-7 dBic	medium	0.95λ×0.95λ×0.1λ
[11]	VSWR>2.5	0	-	simple	1.1λ×1.1λ×0.3λ
This Work	32%	12.7%	7-8 dBic	simple	1.2λ×1.2λ×0.22λ

TABLE II gives a comparison between the proposed antenna and other polarization reconfigurable antennas in terms of impedance bandwidth, overlapped bandwidth, antenna gain and feeding complexity. From this table, it can be seen that the proposed antenna has wider bandwidth and higher gain.

IV. CONCLUSION

A polarization reconfigurable loop antenna with more than 12.7% overlapped bandwidth under both RHCP and LHCP states is proposed in this paper. By controlling the states of the integrated PIN diodes on the loop, the polarization status of the proposed antenna can be changed easily. Compared with other polarization reconfigurable antennas with switchable circular polarization, the proposed antenna has wider bandwidth and higher antenna gain with a simple configuration.

REFERENCES

[1] F. Yang and Y. Rahmat-Samii, "A reconfigurable patch antenna using switchable slots for circular polarization diversity," Microw. Opt. Technol. Lett, vol. 12, pp. 96-98, 2002.
[2] S. Gao, A. Sambell, and S. Zhong, "Polarization-agile antennas," IEEE Antennas Propag. Mag., vol. 48, pp. 28-37, 2006.
[3] P.-Y. Qin, Y. Guo, and C.-H. Liang, "Effect of antenna polarization diversity on MIMO system capacity," IEEE Antennas Wireless Propag. Lett., vol. 9, pp. 1092-1095, 2010.
[4] B. A. Cetiner, E. Akay, E. Sengul, and E. Ayanoglu, "A MIMO system with multifunctional reconfigurable antennas," IEEE Antennas Wireless Propag. Lett., vol. 5, pp. 463-466, 2006.
[5] S. Gao, Q. Luo, and F. Zhu, Circularly polarized antennas: John Wiley & Sons, 2013.
[6] P.-Y. Qin, A. R. Weily, Y. Guo, and C.-H. Liang, "Polarization reconfigurable U-slot patch antenna," IEEE Trans. Antennas Propag., vol. 58, pp. 3383-3388, 2010.
[7] S.-H. Hsu and K. Chang, "A novel reconfigurable microstrip antenna with switchable circular polarization," IEEE Antennas Wireless Propag. Lett., vol. 6, pp. 160-162, 2007.
[8] A. Khidre, K.-F. Lee, F. Yang, and A. Z. Elsherbeni, "Circular polarization reconfigurable wideband E-shaped patch antenna for wireless applications," IEEE Trans. Antennas Propag., vol. 61, pp. 960-964, 2013.
[9] S.-L. S. Yang and K.-M. Luk, "A wideband L-probes fed circularly-polarized reconfigurable microstrip patch antenna," IEEE Trans. Antennas Propag., vol. 56, pp. 581-584, 2008.
[10] H. Scott and V. Fusco, "Polarization agile circular wire loop antenna," IEEE Antennas Wireless Propag. Lett., vol. 1, pp. 64-66, 2002.
[11] R. Li, N. A. Bushyager, J. Laskar, and M. M. Tentzeris, "Determination of reactance loading for circularly polarized circular loop antennas with a uniform traveling-wave current distribution," Antennas and Propagation, IEEE Transactions on, vol. 53, pp. 3920-3929, 2005.
[12] R.-L. Li, V. F. Fusco, and H. Nakano, "Circularly polarized open-loop antenna," IEEE Trans. Antennas Propag., vol. 51, pp. 2475-2477, 2003.
[13] R. Li, A. Traille, J. Laskar, and M. M. Tentzeris, "Bandwidth and gain improvement of a circularly polarized dual-rhombic loop antenna," IEEE Antennas Wireless Propag. Lett., vol. 5, pp. 84-87, 2006.
[14] R. Li, G. DeJean, J. Laskar, and M. M. Tentzeris, "Investigation of circularly polarized loop antennas with a parasitic element for bandwidth enhancement," Antennas and Propagation, IEEE Transactions on, vol. 53, pp. 3930-3939, 2005.
[15] R. Bawer and J. Wolfe, "A printed circuit balun for use with spiral antennas," IRE Trans. Microw. Theory Tech, vol. 8, pp. 319-325, 1960.
[16] B. Y. Toh, R. Cahill, and V. F. Fusco, "Understanding and measuring circular polarization," IEEE Trans. Education, vol. 46, pp. 313-318, 2003.